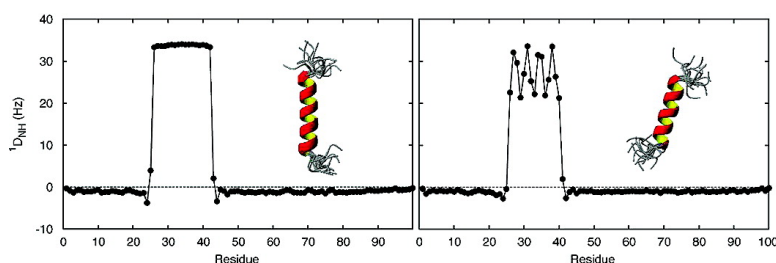


## On the Origin of NMR Dipolar Waves in Transient Helical Elements of Partially Folded Proteins

Malene Ringkjøbing Jensen, and Martin Blackledge

*J. Am. Chem. Soc.*, **2008**, 130 (34), 11266-11267 • DOI: 10.1021/ja8039184 • Publication Date (Web): 30 July 2008

Downloaded from <http://pubs.acs.org> on February 8, 2009



### More About This Article

Additional resources and features associated with this article are available within the HTML version:

- Supporting Information
- Access to high resolution figures
- Links to articles and content related to this article
- Copyright permission to reproduce figures and/or text from this article

[View the Full Text HTML](#)

## On the Origin of NMR Dipolar Waves in Transient Helical Elements of Partially Folded Proteins

Malene Ringkjøbing Jensen and Martin Blackledge\*

*Protein Dynamics and Flexibility by NMR, Institut de Biologie Structurale Jean-Pierre Ebel, CEA; CNRS; UJF UMR 5075, 41 Rue Jules Horowitz, Grenoble 38027, France*

Received May 25, 2008; E-mail: martin.blackledge@ibs.fr

Residual dipolar couplings (RDCs) are powerful reporters of local conformational sampling in intrinsically unfolded or chemically denatured proteins,<sup>1–8</sup> offering a powerful tool for studying molecular recognition and protein folding. Although RDCs have been used to identify transient helical formation within partially folded proteins, quantitative conformational interpretation has remained elusive. Experimental <sup>1</sup>D<sub>NH</sub> RDCs previously measured in the S-peptide of ribonuclease A and N<sub>TAIL</sub> (443–524), the C-terminal domain of the Sendai virus nucleoprotein, are shown in Figure 1. Both peptides contain a helical element sandwiched between unfolded peptide chains, and in each case “dipolar waves” are visible as a periodicity of *i* to (*i*+3) or (*i*+4) in the RDC values within the helical elements (S-peptide: T3-M13, N<sub>TAIL</sub>: V476-A488). Similar periodicity has been observed in <sup>1</sup>D<sub>CαHα</sub>, <sup>1</sup>D<sub>CαC'</sub>, and <sup>2</sup>D<sub>HNC'</sub> couplings in N<sub>TAIL</sub>.<sup>9</sup> Here we identify the origin of this phenomenon and develop a simple and efficient tool to quantify the nature and extent of transient helical elements present in partially folded proteins.

The observation of dipolar or quadrupolar waves within helical elements of folded proteins has been shown to provide recognizable signatures for helical orientation relative to a molecular alignment tensor or lipid bilayer.<sup>10–16</sup> The cause of periodicity of RDCs measured in partially folded chains is less intuitively clear. Assuming that the helix is not deformed, this can only occur if the effective orientation of vectors on either side of the helix differs relative to the field, resulting in an average tilt of the main axis of the helical element in the magnetic field. To clarify this phenomenon, simulations of RDCs in partially unfolded polyalanine chains were performed using *Flexible-Meccano*, an explicit ensemble molecular description applicable to prediction of RDCs in dynamically fluctuating systems. The algorithm generates conformers of unfolded chains using a residue-specific  $\phi/\psi$  database as previously described.<sup>1</sup> The alignment tensor and RDCs for each conformer were calculated using PALES<sup>17</sup> with the following expression:

$$D_{ij} = -\frac{\gamma_i \gamma_j \mu_0 h}{16\pi^3 r_{ij}^3} \left[ A_a (3 \cos^2 \theta - 1) + \frac{3}{2} A_r \sin^2 \theta \cos(2\varphi) \right] \quad (1)$$

where,  $A_a$  and  $A_r$  are the axial and rhombic components of the alignment tensor and ( $r_{ij}$ ,  $\theta$ ,  $\varphi$ ) are the spherical coordinates of the  $ij$  vector in this frame. RDCs were then averaged over the whole ensemble. Helices with different lengths and positions in a 100 amino acid polyalanine chain were introduced by randomly sampling the  $\alpha$ -helical region of  $\phi/\psi$  space ( $-65^\circ$ ,  $-40^\circ$ ) using a Gaussian distribution with a width of  $3^\circ$ . Helices were initiated at position 26 with lengths of 4–40 amino acids. The remaining chain sampled amino acid specific (alanine) backbone dihedral distributions.

Ensemble-averaged RDCs (<sup>1</sup>D<sub>NH</sub>, <sup>1</sup>D<sub>CαHα</sub>, and <sup>1</sup>D<sub>CαC'</sub>) from within the helical element of each of the ensembles were fit to an ideal helical structure using eq 1 by optimizing  $A_a$ ,  $A_r$  and  $\alpha$ ,  $\beta$ ,  $\gamma$  defining the tensor orientation relative to the helix. The fit was essentially perfect in all cases, and  $A_r$  was found to be negligible

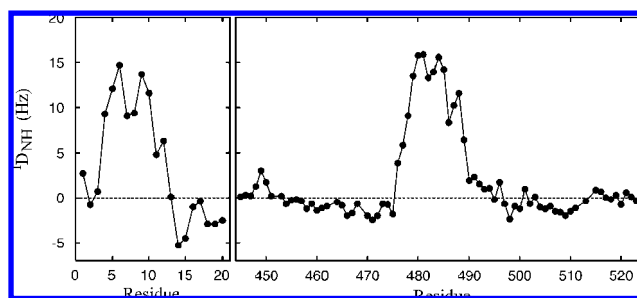


**Figure 1.** Experimental <sup>1</sup>D<sub>NH</sub> measured previously in (left) the S-peptide of ribonuclease A at 0.5 M salt and 0 °C aligned in C8E5 PEG/*n*-octanol<sup>9</sup> and (right) N<sub>TAIL</sub>, the C-terminal domain of Sendai virus nucleoprotein at 50 mM salt and 25 °C aligned in C12E5 PEG/1-hexanol liquid crystals.<sup>10</sup>

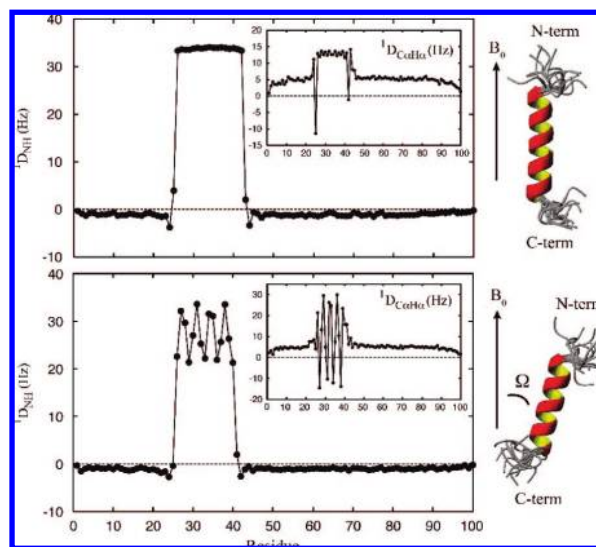


**Figure 2.** <sup>1</sup>D<sub>NH</sub> and <sup>1</sup>D<sub>CαHα</sub> (inserts) calculated for a 100 amino acid poly-Ala chain with helices at 26–41 (top) and 26–39 (bottom). RDCs were averaged over 50 000 conformers. In each case 15 superimposed conformers from *Flexible-Meccano* show the directionality of the unfolded chains projected from the helix caps. For clarity only the first four residues before and after the helix are shown. The effective tilt angle imposed by the helix capping is 1.3° (top) and 18° (bottom).

for each ensemble. Simulated average <sup>1</sup>D<sub>NH</sub> and <sup>1</sup>D<sub>CαHα</sub> couplings are compared for two unfolded polyalanine chains (Figure 2) where helices were introduced at residues 26–39 and 26–41. A difference in length of only two amino acids induces distinctly different dipolar waves. Despite the high flexibility of the long N- and C-terminal chains, the appearance of periodicity in the RDC profile within the helix is strongly correlated with the direction of the unfolded chains as they are immediately projected from the helix ends. If the dynamic chains are projected in the same direction (26–41), dipolar oscillations are small, because the effective orientation of the helix

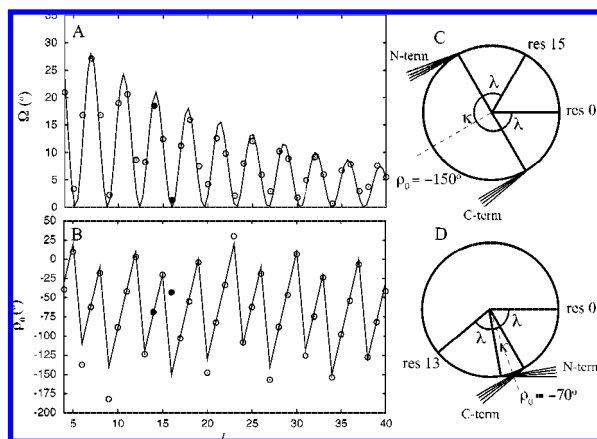


**Figure 3.** Dipolar waves in flexible chains. (A) Effective tilt angle,  $\Omega$ , relative to magnetic field as a function of helix length  $l$  (in residues) introduced between sites 26 and 65 of a 100aa poly ala. RDCs were averaged over 2000 conformers and fit to an ideal helix using eq 2. Line corresponds to the fit of simulated data points with  $\Omega(l) = k_1 \exp(-k_2 l) \cos^2(\kappa(l)/2)$ ;  $\kappa$  is the angle between points of chain projection given by  $\kappa(l) = 360(l - 1)/p + 2\lambda$  (fitted values:  $k_1 = 37.3$ ,  $k_2 = 0.01$ ,  $p$  (periodicity) = 3.6 and  $\lambda = 60$ ). The two simulations in Figure 2 are indicated by filled circles. (B) Helix polarity,  $\rho_0$ , as a function of  $l$ . Circles correspond to values derived from explicit simulation.  $\rho_0$  was obtained by fitting simulated RDCs to eq 2 using an ideal helical structure. Line corresponds to the expected polarity calculated as the average position of the two points of chain projection. The polarity can only be accurately determined for  $\Omega > 4^\circ$ . (C) Top view of helix of length 16 showing the position of the first (res 0) and last (res 15) residues as well as the positions of chain projection. Dashed line indicates expected  $\rho_0$  value. (D) Top view of helix length 14. These helices correspond to the two simulations in Figure 2.

is close to parallel to the field. If the chains are projected in opposing directions (26–39), large oscillations are observed due to the large effective tilt of the helix.

Simulation thus predicts that two features will be expected to vary periodically with respect to the number of amino acids in the helix: the effective tilt ( $\Omega$ ) of the helix axis relative to the alignment frame and the polarity,  $\rho_0$ , describing the angular position of the helix relative to this axis (Figure 3).

Adapting expressions developed in the context of folded proteins,<sup>10–14</sup> RDCs from helical elements present in an unfolded chain can then be calculated as follows:

$$D_{ij} = -\frac{\gamma_i \gamma_j \mu_0 h}{16\pi^3 r_{ij}^3} [A_a (3(\cos \Omega \cos \delta - \sin \Omega \sin \delta \cos(\rho - \rho_0))^2 - 1)] \quad (2)$$

where  $\delta$  is the orientation of the vector relative to the helix axis and  $\rho$  ( $= 2\pi n/3.6$  with  $n = 0, 1, \dots, l - 1$ ) is the position of the individual residue along the helix. Not surprisingly the dependence of  $\Omega$  and  $\rho_0$  on helix length can be parametrized using simple periodic functions (Figure 3). Equation 2 can then be used to calculate expected RDC distributions (dipolar waves) for helices of any length, replacing the time-consuming task of simulating values from explicit ensembles.

In addition to providing an efficient tool for prediction of dipolar waves within helical elements of partially folded proteins, the observed periodicity in both  $\Omega$  and  $\rho_0$  also reveals the origin of dipolar waves in this type of protein. While  $\Omega$  governs the amplitude of the observed dipolar waves, the polarity  $\rho_0$  is the phase of the observed wave. Both parameters report on the directionality and behavior of the neighboring flexible chains and can be used to probe the conformational properties of the unfolded region simply by analyzing the values measured within the helical element.

The influence of the unfolded chain on the effective helix alignment depends on the persistence length over which the conformational sampling of a given vector remains affected by near neighbors. To estimate this range we used *Flexible-Meccano* to predict RDCs from a single helical element within unfolded polyaniline chains of increasing length. Only small changes were observed in fitted  $\Omega$  values for chains longer than six amino acids from the helix termini (Supporting Information), while  $\rho_0$  converged after only three amino acids.

In conclusion, we have used extensive sampling of explicit conformational ensembles to provide new insight into the origin of dipolar waves measured in helical elements present in partially folded proteins. We find that the effective helix tilt and polarity determine the observed periodicity of RDCs within the helix and that observed dipolar waves originate from directional asymmetry in the capping motifs beyond the N and C termini of the helix. RDCs measured within the helix therefore report directly on the behavior of the neighboring capping strands. In analogy to recent developments in solution and solid state NMR of folded proteins, the simple periodic nature of the dipolar wave allows the development of analytical expressions that reproduce the helical RDCs within the flexible chain. This will considerably reduce computational costs incurred when simulating explicit conformational ensembles and provide a portable tool for investigating helix nucleation and fraying in the context of partially folded proteins. The insight derived here will also contribute to the use of RDCs to understand the molecular basis of the initial steps of protein folding.

**Acknowledgment.** This work was supported by the Commissariat à l'Énergie Atomique, the French CNRS, the Université Joseph Fourier, Grenoble, and through ANR NT05-4\_42781. M.R.J is supported by Lundbeckfonden and is a recipient of a long-term EMBO fellowship.

**Supporting Information Available:** Tables containing the fitted  $\Omega$ ,  $\rho_0$ , and  $A_a$  values as function of the helix length. Figure showing the convergence of  $\Omega$  and  $\rho_0$  for a single helical element within unfolded chains of increasing length. Figure showing the application of the approach to the dipolar wave of  $N_{TAIL}$ . This material is available free of charge via the Internet at <http://pubs.acs.org>.

## References

- Bernado, P.; Blanchard, L.; Timmins, P.; Marion, D.; Ruigrok, R. W. H.; Blackledge, M. *Proc. Natl. Acad. Sci. U.S.A.* **2005**, *102*, 17002–17007.
- Jha, A. K.; Colubri, A.; Freed, K.; Sosnick, T. *Proc. Natl. Acad. Sci. U.S.A.* **2005**, *102*, 13099–13104.
- Meier, S.; Grzesiek, S.; Blackledge, M. *J. Am. Chem. Soc.* **2007**, *129*, 9799–9807.
- Meier, S.; Blackledge, M.; Grzesiek, S. *J. Chem. Phys.* **2008**, *128*, 052204.
- Bernado, P.; Bertocini, C.; Griesinger, C.; Zweckstetter, M.; Blackledge, M. *J. Am. Chem. Soc.* **2005**, *127*, 17968–17969.
- Mohana-Borges, R.; Goto, N. K.; Kroon, G. J. A.; Dyson, H. J.; Wright, P. E. *J. Mol. Biol.* **2004**, *340*, 1131–1142.
- Fieber, W.; Kristjansdottir, S.; Poulsen, F. M. *J. Mol. Biol.* **2004**, *339*, 1191–1199.
- Alexandrescu, A. T.; Kammerer, R. A. *Protein Sci.* **2003**, *12*, 2132–2140.
- Jensen, M. R.; Houben, K.; Lescep, E.; Blanchard, L.; Ruigrok, R. W. H.; Blackledge, M. *J. Am. Chem. Soc.* **2008**, *130*, 8055–8061.
- Marassi, F. M.; Opella, S. J. *J. Magn. Reson.* **2000**, *144*, 150–155.
- Mesleh, M. F.; Lee, S.; Veglia, G.; Thiriot, D. S.; Marassi, F. M.; Opella, S. J. *J. Am. Chem. Soc.* **2003**, *125*, 8928–8935.
- Mesleh, M. F.; Veglia, G.; DeSilva, T. M.; Marassi, F. M.; Opella, S. J. *J. Am. Chem. Soc.* **2002**, *124*, 4206–4207.
- Mascioni, A.; Veglia, G. *J. Am. Chem. Soc.* **2003**, *125*, 12520–12526.
- Mesleh, M. F.; Opella, S. J. *J. Magn. Reson.* **2003**, *163*, 288–299.
- Walsh, J. D.; Cabello-Villegas, J.; Wang, Y. X. *J. Am. Chem. Soc.* **2004**, *126*, 1938–1939.
- Strandberg, E.; Ozdirekcan, S.; Rijkers, D. T. S.; van der Wel, P. C. A.; Koeppe, R. E.; Liskamp, R.; Killian, J. A. *Biophys. J.* **2004**, *86*, 3709–3721.
- Zweckstetter, M.; Bax, A. *J. Am. Chem. Soc.* **2000**, *122*, 3791–3792.

JA8039184